



are (i) air quality management for reduction of pollution and healthy environment [1-2] and (ii) automation of public buildings for reducing human effort and energy consumption [3]. There have been numerous efforts on microclimate monitoring using Wireless Sensor Network (WSN). In [2-4] authors report indoor air quality monitoring by measuring pollution levels for indoor environments. In [5] author attaining energy autonomy for sensor node. In day to day life, humans interact with environmental parameters like temperature, humidity, light etc. and try to regulate them manually. Monitoring of these parameters through WSN, makes the system suitable without major modifications in the infrastructure. Such monitoring system for home automation, a part of building automation provides people comfort, security as well as option of energy saving by monitoring the daily energy consumption.

A system which integrates IoT with home monitoring system is discussed in [6]. The WSN based home monitoring system for determining wellness of elderly by monitoring their daily activities is discussed in [7-9]. In [10-11], authors discuss a customized middleware developed for ambient intelligence applications such as home automation. Further to this, a smart power monitoring and controlling system for household appliances is implemented in [12-16] for building automation.

This paper proposes a customized IoT enabled wireless sensing and monitoring platform (IoT-WSMP) that monitors temperature, humidity and light which are essential parameters for building automation. A Graphical User Interface (GUI) that provides a graph for the parameters with continuous monitoring and recording of data is developed in LabVIEW. The recorded data is useful for further analysis and can be useful for controlling the building environment. The Android application proves useful for remote monitoring.

This paper is organized as follows. Section 2 presents the architecture of the proposed WSN and the methodology used for sensing and data transmission. Section 3 reports the experimental results derived during the implementation and validation of the presented system, through its deployment. Section 4 concludes this paper and provides some prospective on potential for future work.

## 2. System Description

The proposed IoT-WSMP consists of a transmitter node, repeater node and a sink node (receiver node) as shown in Fig. 1. The sensing platform supports a one way communication from the transmitter to the receiver node and can accommodate more repeater nodes, if required, to cover a larger area. Furthermore, the proposed system uses a custom hopping method for transmission over a number of nodes. This customised hopping method is simple and scalable. Finally, the data received at the sink node is transferred to a PC through a USB interface. The sensed data is depicted graphically and recorded in an excel sheet through a customized GUI, which is developed in LabVIEW. This data is then transmitted to a MySQL database via PC connected to the internet. The PHP API execution, on internet enables transfer of data from the MySQL database to the android based smart phone, thereby enabling IoT based applications.

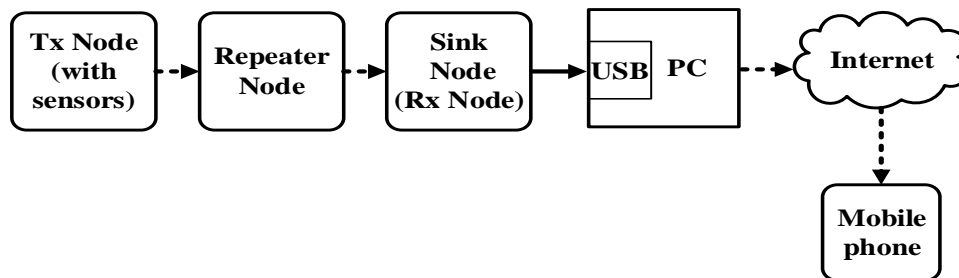


Fig. 1. Proposed System block diagram

### 2.1. Node

The proposed wireless sensor node consists of a temperature and humidity sensor, a light sensor, an ultra-low power microcontroller and a wireless transceiver as shown in Fig. 2. The temperature, humidity and light readings

are processed by the  $\mu$ controller and transmitted through the wireless transceiver. The repeater and receiver nodes have the same components except the on-board sensors. Data sensing and aggregation on the node can be configured by a customized software code and is dependent on the application. Further to this, a custom voting algorithm is implemented to increase data reliability. This algorithm reduces ambiguity in data up to a certain extent and is discussed in detailed in the results section. Power is supplied to the wireless sensor node and repeater node by two AA batteries, while the receiver node attached to a PC is powered through the USB interface.

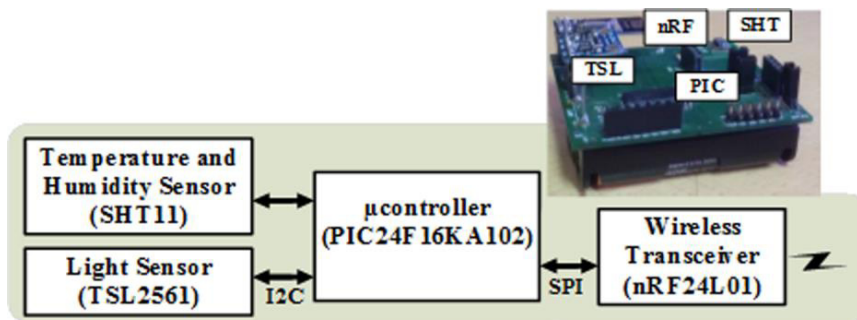


Fig. 2. Proposed Wireless Sensor Node

### 2.1.1 Sensor

The on-board temperature and humidity sensor SHT11 provides a fully calibrated digital output and can be treated as a golden standard [17]. This is also verified with various other standard instruments in laboratory conditions. The sensor has an operating range of  $-40^{\circ}\text{C}$  to  $\pm 123.8^{\circ}\text{C}$  for temperature and 0 to 100% RH for relative humidity. It has an accuracy of  $\pm 0.4^{\circ}\text{C}$  for temperature and  $\pm 3\%$  RH for relative humidity, which is useful for many indoor applications. The sensor has an operating voltage range of 2.4 to 5.5 V that can be used in applications having low power requirements. The sensor has very fast response time and typically needs 11 ms to be in an active state from the power down state. After each measurement, it automatically switches over to a sleep mode with low current requirements. The sensor has a two wire serial interface with a resolution of 14 bit for temperature and 12 bit for humidity.

Table 1. Current Consumption of Sensors

| Module           | Voltage | Mode               | Current               |
|------------------|---------|--------------------|-----------------------|
| Sensor (SHT11)   | 3.3 V   | Measuring          | 0.55-1.0mA            |
|                  |         | Sleep              | $\sim 0.3\mu\text{A}$ |
| Sensor (TSL2561) | 3.3 V   | Measuring (Active) | 0.24-0.6mA            |
|                  |         | Power Down         | 3.2-15 $\mu\text{A}$  |

The second on-board sensor is a TSL2561 sensor from TAOS, which measures the light intensity into a digital output, available through I2C or SMBus interface. It has an operating voltage from 2.7V to 3.6V that measures light intensity from 0.1 to 30,000 lux. The two internal photo diodes can be useful for visible and infrared light conditions. A 16 bit ADC output in the sensor is sufficient for indoor applications. The actual value of intensity is obtained from the digital value by applying empirical formulas [18]. Table 1 shows the current consumption of both the sensors.

### 2.1.2 Microcontroller

The on-board PIC24F16KA102 micro- controller is a 16 bit microcontroller from Microchip, with extreme low power (XLP) technology and consumes nano watts of power. It can run on different power management modes such as run, idle, doze, sleep and deep sleep, making it ideal for running low power algorithms for WSN applications. The operating voltage range is from 1.8V to 3.6V. Table 2 shows the current consumption of the  $\mu$ controller for different states of operation [19].

Table 2. Current Consumption of Microcontroller

| Module                             | Voltage | Mode         | Current     |
|------------------------------------|---------|--------------|-------------|
| Microcontroller<br>(PIC24F16KA102) | 3.3 V   | Active@32MHz | 11-18 mA    |
|                                    |         | Deep Sleep   | 0.55-0.75µA |

2.1.3 Wireless Transceiver

An ultra-low power nRF24L01 from Nordic [20] is used as a radio unit of the sensor node. This transceiver can operate from 1.9V to 3.6V at 2.4-2.5 GHz ISM band and therefore satisfies the constraints for indoor applications. The transceiver interfaces the µcontroller through a 4-wire, Serial Peripheral Interface (SPI) and has different modes of operation like Transmitter (TX) mode, Receiver (RX) mode, two Standby modes and a Power Down mode. Table 3 shows the power consumption of each mode of operation. Also as shown in Fig. 3(a) and (b), the transceiver operates in Shock Burst and Enhanced Shock Burst modes. In Enhanced Shock Burst mode, the receiver sends an acknowledgement to the transmitter after receiving the data, which enables the detection of data loss. In Shock Burst mode, the preamble and CRC of the data packet is generated automatically. Also, unlike in Enhanced Shock Burst mode, it eliminates the need for 9 flag bits and therefore demands less memory. Furthermore, Shock Burst mode allows lower data rate with reduction in average current consumption and therefore it is the preferred mode in our proposed work. The transceiver nRF24L01 can be configured to receive data from as many as the six different transmitters through as many as six different data pipes, each having its own unique address. In the proposed system only two data pipes are sufficient, i.e. Pipe-0 for transmission between transmitter and repeater node and pipe-1 between repeater and receiver node.

Table 3. Current Consumption of Transceiver

| Module                    | Voltage | Mode            | Current |
|---------------------------|---------|-----------------|---------|
| Transceiver<br>(nRF24L01) | 3.3 V   | TX mode (0 dBm) | 11.3mA  |
|                           |         | RX mode(2Mbps)  | 12.3mA  |
|                           |         | Power Down mode | 900nA   |
|                           |         | Standby-I mode  | 32µA    |

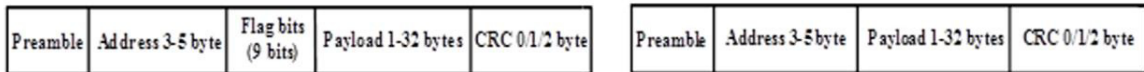


Fig. 3: (a) Enhanced Shock Burst Packet format

(b) Shock Burst packet format

The above selected µcontroller, transceiver and sensors provide an added advantage of operating all of them at a single voltage (3.0V), without the need for an expensive DC-DC conversion.

2.2 Methodology for Sensing and Transmission

The operation of the WSN node consists of two phases; (i) sensing and (ii) transmission. Table 4 shows the different states of the individual components. The bottom most row of the Table 4 shows the duration of time for which the modules are active in those states. For example, in state S1, the microcontroller is active for 1 ms, whereas all other modules (nRF24L01, SHT11, TSL2561) are in sleep state. The graphical representation of the states is also shown in Fig. 4, depicting the time duration and current consumption of the sensor node in different states. This provides an intuitive representation to optimize the operation of the sensor node depending upon the power requirement of the application.

Initially, switching on the power automatically puts the transmitter node in state S1, where it stays for 1 ms. The node is programmed such that it immediately enters state S2. It remains in this state for 400 ms during which time, SHT11 is setup and data is written to the µcontroller memory. The duration of state S3 is also of 400 ms during which TSL2561 is setup, intensity data is measured and the sensor is switched to standby mode. After 1 sec, states S2 to S6 are repeated twice in state S7. In state S7, after the three sets of data are written to the

µcontroller memory, a voting algorithm is performed to remove anomalies, if any. By doing so, the reliability of the data is enhanced and is shown in the results section.

Table 4. Duration of Different States of the wireless Sensor Node

| Modules/States | S1      | S2      | S3                | S4      | S5         | S6      | S7       | S8     |
|----------------|---------|---------|-------------------|---------|------------|---------|----------|--------|
| µcontroller    | Active  | Active  | Active            | Active  | Active     | Active  | S2 to S6 | Active |
| Transceiver    | Standby | Standby | Standby           | Standby | Standby    | Standby | repeated | Active |
| SHT11          | Sleep   | Active  | Sleep             | Sleep   | Sleep      | Sleep   | twice    | Sleep  |
| TSL2561        | Sleep   | Sleep   | Power Up          | Active  | Power Down | Sleep   |          | Sleep  |
| Time Duration  | 1 ms    | 400 ms  | 400 ms (S3+S4+S5) |         |            | 1 sec   |          | 235 µs |

For transmission, it is assumed that data at sensor node is sent at every 5.4 secs. Based on this assumption, for the purpose of convenience and reliability, the duration of the reception for a single transmission is set, longer than the 5.4 secs. At the receiver node, a duration of 6 secs is set for receiving three data points at an interval of 2 secs. This is kept less frequent than the repeater node, based on the results of experiments. The customised double hopping algorithm ensures that the receiver chooses the right data packet from the number of received data packets and thereby increases the reliability of the system.

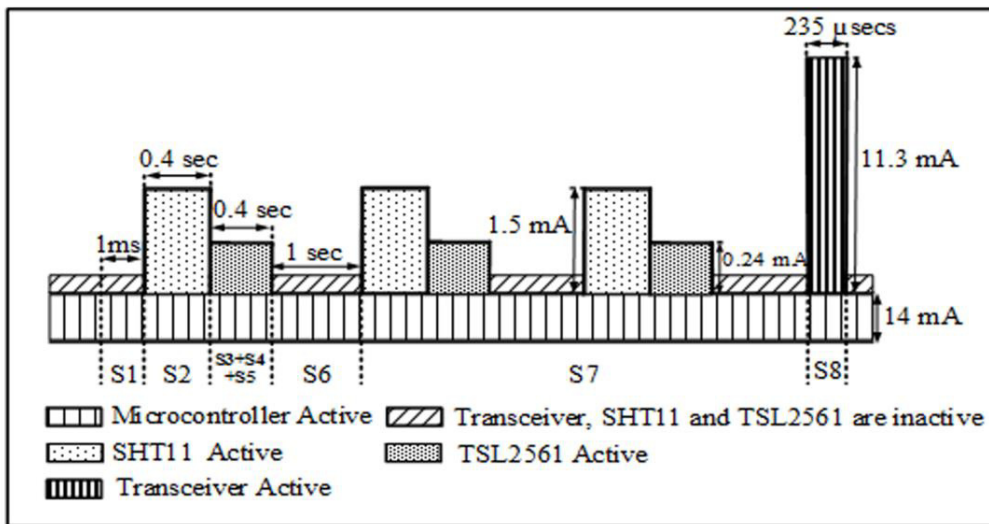


Fig. 4: State Diagram for the Sensor Node

However, reliability is increased at slightly higher power consumption as discussed in the experimental results. Furthermore, with the above sensing and transmission scheme, it is possible to quantify, in terms of power and time, the various states of the WSN at ease. This provides a scope to further optimization for future deployments. For example, if S1 is stretched during the sleep mode, the average power consumption is lowered, thereby prolonging the battery life. This is also explained and quantified in the experimental results.

To measure the current of each individual module of the sensor node that particular module was kept active for a fixed duration and the current was obtained by the standard digital multimeter setup. Table 5 shows the power calculations for the sensor node. For different states, total current is calculated by adding currents of all modules, according to their states as stated in Table 5. For each state, the final value of the time is obtained by multiplication of time and repetition of time. For example, for state S2, final value of time is 0.4 sec multiplied by 3. Energy for different states is calculated by multiplication of total current, voltage and final value of time. Total energy is the summation of energy of all the states of the node. Total time calculated by summation of final value of time for all states is 5.4 secs. The average power of the sensor node is calculated by dividing the total energy by the total time period, and the result obtained is 43.25 mW.

Table 5. Power calculation for the Sensor Node

| Modules              | Current (mA) for different states |        |          |        |         |
|----------------------|-----------------------------------|--------|----------|--------|---------|
|                      | S1                                | S2     | S3+S4+S5 | S6     | S8      |
| Microcontroller      | 14                                | 14     | 14       | 14     | 14      |
| Transceiver          | 32e-3*                            | 32e-3  | 32e-3    | 32e-3  | 11.3*   |
| SHT11                | 1e-5                              | 1.5    | 1e-5     | 1e-5   | 1e-5    |
| TSL2561              | 3.2e-3*                           | 3.2e-3 | 0.24*    | 3.2e-3 | 3.2e-3  |
| Total I (mA)         | 14.03                             | 15.53  | 14.27    | 14.03  | 25.30   |
| Time (sec)           | 1e-3                              | 0.4    | 0.4      | 1      | 2.35e-4 |
| Repetition of time   | 1                                 | 3      | 3        | 3      | 1       |
| Voltage              | 3                                 | 3      | 3        | 3      | 3       |
| Energy (mJ)          | 0.04                              | 55.90  | 51.37    | 126.27 | 0.017   |
| Total Energy (mJ) =  | 233.59                            |        |          |        |         |
| Total Time (secs) =  | 5.40                              |        |          |        |         |
| Average Power (mW) = | 43.25                             |        |          |        |         |

\*Estimated current

### 2.3 Graphical User Interface

A graphical panel of GUI made in LabVIEW is developed as shown in Fig. 5(a). The data is displayed in both graphical and numeric form. Virtual Instrument Software Architecture (VISA) API is used to interface sink node with Lab- VIEW. VISA is a standard I/O API for instrumentation programming. It is a standard for configuring, programming and troubleshooting instrumentation systems comprising GPIB, VXI, PXI, Serial, Ethernet, and/or USB interfaces. VISA is adopted as it is interface independent. The monitored data is stored in excel sheet with current date and time. In the front panel, the user can interrupt the setup and can configure the system setup. The programming is developed in such a way that the excel sheet stores the actual time of sensing instead of delayed time.

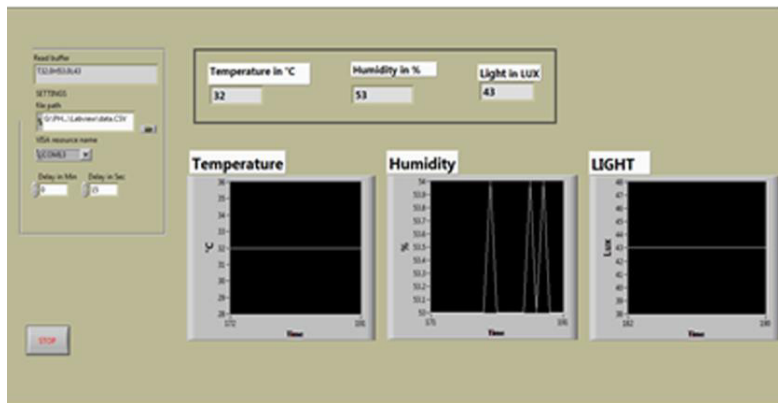
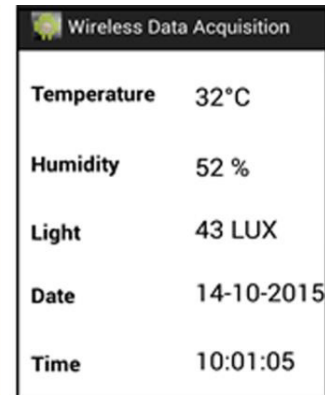


Fig. 5. (a) Graphical user interface



(b) Android Application.

### 2.4 Android Application

Further, to enable IoT, the monitored data in LabVIEW is transferred to MySQL database server through internet. PHP API executes on the internet server. It connects to the MySQL database and returns the data in plain HTML page in Java Script Object Notation (json), according to the query defined in it. An android application is developed in the Eclipse IDE using java. Internet connection permissions are given in it to connect with Wi-Fi. Data from the database (located in MySQL) can be obtained on the mobile phone by clicking the developed android application on the mobile phone. When the android program is clicked, it connects to URL of PHP API. As a result

PHP API connects with the database and returns the data to the mobile phone. Fig. 5(b) shows the screen shot of the developed android application. The developed android application is tested on a smart phone based on android 4.3.

### 3 Experimental results and deployment

The proposed system is validated by carrying out experiments in the laboratory. In ten different light intensity environments, ten different results for the TSL2561 sensor are logged and ten results of lux meter from Metravi, 1330 are manually recorded. Considering lux meter reading as a true value, obtained minimum and maximum value of relative error are 1.74% and 10.68% respectively. So it can be considered that TSL2561 readings are in close agreement with the actual values.

Deployment of the proposed system in the laboratory is done by placing the sensor node and router node in the same room (at a distance of 4.75m from each other) and sink node in another room (at a distance of 3.75m from router node) so that they are separated by walls, creating real environment such as in buildings.

For this deployment, Fig. 6(a) shows the filtered results for the implemented IoT based monitoring system for one hour duration. In the results temperature is in Celsius, relative humidity is in % and light is in lux. The reliability is obtained by transmitting data from TX node at the interval of 12 secs and receiving data from RX node. For this deployment, reliability obtained is 99.6%, as from 1000 data at RX node 996 data are received correctly as shown in Table 6.

Table 6. Reliability of Data Transmission

| Time between two samples | Expected Number of packets | Number of correctly received packets | Reliability (%) |
|--------------------------|----------------------------|--------------------------------------|-----------------|
| 12 secs                  | 1000                       | 996                                  | 99.6            |

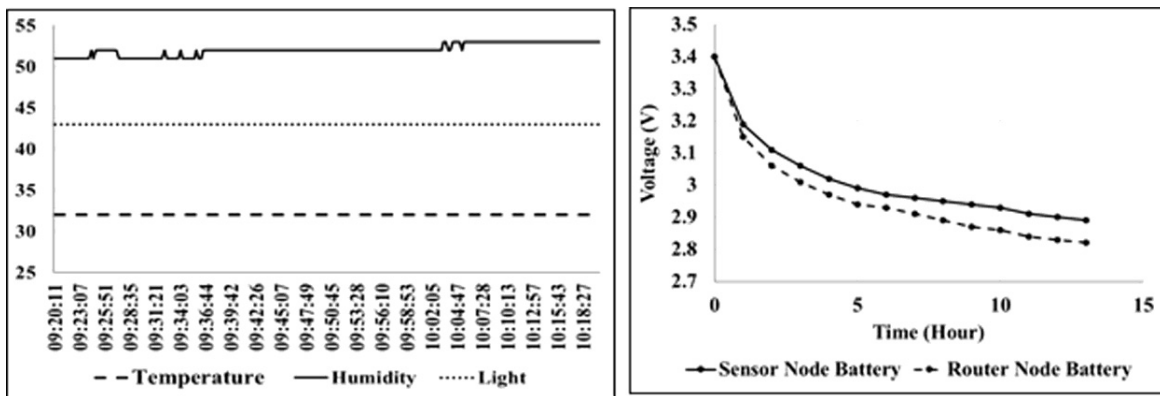


Fig. 6. (a) Temperature Humidity and Light Results

(b) Battery voltage results of the Sensor and Repeater Node

Battery voltage of the sensor node and repeater node are measured using a multimeter at intervals of one hour over a period of thirteen hours. As shown in Fig. 6(b) the battery voltage drop out is high initially and then after a particular duration it is 0.01V for each hour, with an occasional reading of 0.02V in some hours. Observing the initial dropout and final voltage of the battery over a period of thirteen hours shows that the battery dropout voltage of the router node is higher than that of the transmitter node. Higher power consumption of the repeater node is because of the methodology used for transmission, for getting higher reliability. After thirteen hours, battery voltage of the sensor node reaches 2.89V. With this drop of 0.51V in 13 hours, the battery discharging 1200mAh has an energy consumption of 7956mJ. To calculate the estimated life time of the node, the total voltage drop is taken to be 0.7V, at which the node stops functioning reliably. The energy consumption of the transmitter node at 0.7V with 1200mAh when divided with the average power consumption (Table 5), gives the estimated life time of the sensor node and is roughly about 20 hours. Based on the estimation and the state diagram (Fig 4), by increasing the duration of the state S1, the battery lifetime can be prolonged.

#### 4 Conclusion and future work

The developed IoT-WSMP system for monitoring temperature, relative humidity and light with double hopping has been successfully implemented and validated in a building environment. A high reliability of 99.6 % is obtained through customized double hopping method. The average power consumption of the transmitter node is 43.25 mW. The developed android application is tested on a smart phone based on android 4.3. Further power reduction is possible through algorithms, hardware optimizations and coding techniques and is dependent on specific application study and is left as future work.

#### Acknowledgement

Authors thank the Gujarat Council of Science and Technology (DST), Gandhinagar for financial support under grant reference GUJCOST/MRP/2014-15/2582.

#### References

- [1] Zanella, N. Bui, A. Castellani, L. Vangelista, and M. Zorzi, "Internet of Things for Smart Cities," IEEE Internet of Things, vol. 1, no. 1, pp. 22–32, 2014.
- [2] S. C. Folea and G. Mois, "A Low-Power Wireless Sensor for Online Ambient Monitoring," IEEE Sensors Journal, vol. 15, no. 2, pp. 742–749, 2015.
- [3] D. Brunelli, I. Minakov, R. Passerone, and M. Rossi, "POVOMON: An Ad-hoc Wireless Sensor Network for indoor environmental monitoring," 2014 IEEE Work- shop on Environmental, Energy, and Structural Monitoring Systems Proceedings, pp. 1–6, 2014.
- [4] P. Changhai, Q. Kun, and W. Chenyang, "Design and Application of a VOC- Monitoring System Based on a ZigBee Wireless Sensor Network," IEEE Sensors Journal, vol. 15, no. 4, pp. 2255–2268, 2015.
- [5] B. Mishra, C. Betterton, G. Tasselli, C. Robert, P. A. Farina, P. Janphuang, D. Briand, and N. F. de Rooij, "A sub 100µw uwb sensor-node powered by a piezoelectric vibration harvester," in Wireless Information Technology and Systems (ICWITS), 2012 IEEE International Conference on. IEEE, 2012, pp. 1–4.
- [6] S. D. T. Kelly, N. K. Suryadevara, and S. C. Mukhopadhyay, "Towards the implementation of IoT for environmental condition monitoring in homes," IEEE Sensors Journal, vol. 13, no. 10, pp. 3846–3853, 2013.
- [7] N. K. Suryadevara, S. Member, and S. C. Mukhopadhyay, "System for Wellness Determination of Elderly," IEEE Sensor Journal, vol. 12, no. 6, pp. 1965–1972, 2012.
- [8] S. Helal, W. Mann, H. El-Zabadani, J. King, Y. Kaddoura, and E. Jansen, "The Gator tech smart house: A programmable pervasive space," Computer, vol. 38, no. 3, pp. 50–60, 2005.
- [9] L. C. De Silva, C. Marikina, and I. M. Petra, "State of the art of smart homes," Engineering Applications of Artificial Intelligence, vol.25, no.7, pp.1313–321, 2012.
- [10] M. Eisenhauer, P. Rosengren, and P. Antolin, "A development platform for integrating wireless devices and sensors into Ambient Intelligence systems," 6th IEEE Annual Communications Society Conference on Sensor, Mesh and Ad Hoc Communications and Networks Workshops, SECON Workshops 2009, vol. 00, no. c, pp. 1–3, 2009.
- [11] Surie, Dipak, Olivier Laguionie, and Thomas Pederson, "Wireless sensor networking of everyday objects in a smart home environment." Intelligent Sensors, Sensor Networks and Information Processing, 2008. ISSNIP 2008. International Conference on. IEEE, 2008.
- [12] N. K. Suryadevara, S. C. Mukhopadhyay, S. D. T. Kelly, and S. P. S. Gill, "WSN-Based Smart Sensors and Actuator for Power Management in Intelligent Buildings," IEEE/ASME Transactions on Mechatronics, vol. 20, no. 2, pp. 564–571, 2015.
- [13] N. Skeledzija, J. Cesic, E. Koco, V. Bachler, H. N. Vucemilo, and H. Dzapov, "Smart home automation system for energy efficient housing," 2014 37th International Convention on Information and Communication Technology, Electronics and Microelectronics (MIPRO), no. May, pp. 166–171, 2014.
- [14] Sankaranarayanan, Sriram, and Au Thien Wan, "ABASH—Android based smart home monitoring using wireless sensors." Clean Energy and Technology (CEAT), 2013 IEEE Conference on. IEEE, 2013.
- [15] M.T. Vo, V.S. Tran, T. D. Nguyen, and H.-T. Huynh, "Wireless Sensor Network for multi-storey building: Design and implementation," 2013 International Conference on Computing, Management and Telecommunications (ComManTel), pp. 175–180, 2013.
- [16] J. Byun, B. Jeon, J. Noh, Y. Kim, and S. Park, "An intelligent self-adjusting sensor for smart home services based on ZigBee communications," IEEE Transactions on Consumer Electronics, vol. 58, no. 3, pp. 794–802, 2012.
- [17] Sensirion, SHT1x datasheet. [Online]. Available: <http://www.sensirion.com>
- [18] Texas Advanced Optoelectronic Solutions, TSL2560, TSL2561, Light-To-Digital Converter. [Online]. Available: <http://www.taosinc.com>
- [19] Microchip Technology, PIC24F16KA102 Family Data Sheet 16-Bit Flash Microcontrollers with Nano Watt XLP Technology. [Online]. Available: <http://www.microchip.com>
- [20] Nordic Semiconductor, Single chip 2.4GHz Transceiver nRF24L01. [Online]. Available: <http://www.nordicsemi.com>.